Field-induced incommensurate order for the quasi-one-dimensional *XXZ* model in a magnetic field

Kouichi Okunishi[1] and Takahumi Suzuki[2]
[1]*Department of Physics, Niigata University, Niigata 950-2181, Japan*
[2]*Institute for Solid State Physics, University of Tokyo, Kashiwa, Chiba 277-8581, Japan*
(Received 2 October 2007; published 14 December 2007)

We investigate phase transitions of the quasi-one-dimensional $S=1/2$ *XXZ* model in a magnetic field, using bosonization combined with a mean-field treatment of the interchain interaction. We then find that the field-induced incommensurate order is certainly realized in the low-field region, while transverse staggered order appears in the high-field region. On the basis of the result, we discuss the field-induced phase transition recently observed for $BaCo_2V_2O_8$.

DOI: 10.1103/PhysRevB.76.224411 PACS number(s): 75.10.Jm, 75.30.Kz, 75.40.Cx

I. INTRODUCTION

Field-induced phase transitions in quantum spin systems have been providing interesting physics, such as magnon Bose Einstein condensation.[1] Recently, an exotic field-induced phase transition was observed for $BaCo_2V_2O_8$,[2] which can be regarded as a quasi-one-dimensional (1D) $S=1/2$ *XXZ* antiferromagnt having Ising-like anisotropy $\Delta \simeq 2$; magnetization and electron spin resonance (ESR) measurements above 1.8 K show that $BaCo_2V_2O_8$ is basically described by the Bethe-ansatz-based theoretical analysis.[3] However, specific heat measurements up to 12 T below 1.8 K reveal that the weak 3D couplings possibly trigger an exotic incommensurate (IC) order in the low-field region.[4] A peculiar point about this phase is that the ordering is different from the Néel type at zero magnetic field, and the shape of the phase boundary in the *H-T* plane is quite different from the usual field-induced order in the coupled Haldane system.[5] This suggests that the Ising-like anisotropy in the quasi-1D system plays an essential role in the field-induced IC order phase, behind which there is substantially important physics.

The 1D *XXZ* antiferromagnet is an exactly solved model playing the essential role to understand the critical quantum fluctuation and strong correlation effects.[6–8] Although the Ising-like anisotropy favors z-directed Néel (z Néel) order at zero magnetization, the magnetic field beyond the critical field H_c recovers the critical quantum fluctuation (see Fig. 1) and then the system is described as a Tomonaga-Luttinger (TL) liquid,[7] which is characterized by power-law decay of the correlation functions:

$$\langle S_n^z S_0^z \rangle = M_z^2 - \frac{1}{4\pi^2 \eta n^2} + A_1 \frac{\cos 2k_F n}{|n|^{1/\eta}} \cdots , \tag{1}$$

$$\langle S_n^x S_0^x \rangle = (-1)^n \left(B_0 \frac{1}{|n|^{\eta}} - B_1 \frac{\cos 2k_F n}{|n|^{\eta+1/\eta}} \cdots \right), \tag{2}$$

where η is the TL exponent, M_z is the uniform magnetization due to a magnetic field H, and the corresponding Fermi wave number is $k_F \equiv \pi(1/2 - M_z)$. The nonuniversal coefficients A and B were evaluated in Ref. 9. For the isotropic Heisenberg model, $\eta < 1$ is always satisfied and thus the transverse fluctuation of (2) is dominant. For the Ising-like case, however, $\eta > 1$ appears in the low-field region, where the longitudinal IC fluctuation becomes dominant. In the actual quasi-1D compound, there is necessarily interchain interaction, which may bring a finite-temperature phase transition accompanying the field-dependent IC order.

In this paper, we investigate the field-induced IC order for coupled *XXZ* chains, using bosonization combined with a mean-field treatment of the interchain interaction.[10] In particular, we make a quantitative analysis of the transition temperatures, taking account of the nonuniversal coefficients in (1) and (2). We then find that the IC order is certainly realized in the low-field region, in contrast with Ref. 11, where the possibility of IC order was not taken into account, while transverse staggered order appears in the high-field region. Moreover, we show that the present theory successfully explains the field dependence of the experimentally observed transition temperature. We also determine the interchain coupling of $BaCo_2V_2O_8$ as 0.09 K.

This paper is organized as follows. In Sec. II, we explain the model and the mean-field theory for the interchain interaction on the basis of bosonization. In Sec. III, the magnetic-field dependences of the transition temperatures are presented for the IC order and the transverse staggered order. Then the IC order of $BaCo_2V_2O_8$ is discussed in detail. In Sec. IV, we summarize our conclusions and discuss related topics.

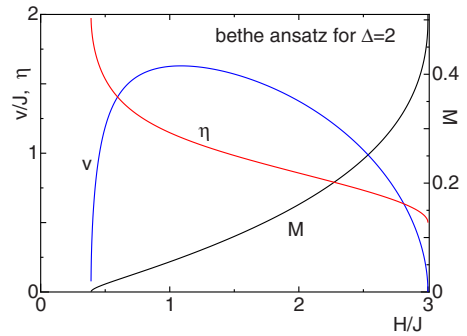

FIG. 1. (Color online) Exact magnetization curve M, critical exponent η, and spin wave velocity v for the *XXZ* chain of $\Delta=2$.

II. MODEL AND FORMULATION

The relevant model we consider here is weakly coupled $S=1/2$ XXZ chains on a simple cubic lattice; its Hamiltonian is given by

$$\mathcal{H}=\sum_{n,j} J(\boldsymbol{S}_{n,j}\cdot\boldsymbol{S}_{n+1,j})_\Delta+\sum_{n,\langle j,j'\rangle} J'(\boldsymbol{S}_{n,j}\cdot\boldsymbol{S}_{n,j'})_\Delta-H\sum_{n,j} S^z_{n,j}, \tag{3}$$

where $(\boldsymbol{S}\cdot\boldsymbol{S})_\Delta\equiv S^xS^x+S^yS^y+\Delta S^zS^z$ is the deformed inner product. The index n runs along the chain direction, j labels the interchain direction, and $\langle j,j'\rangle$ denote the nearest-neighbor pairs of the chains. Then J is the exchange coupling along the chain direction and the interchain interaction is controlled by J' ($\ll J$). Note that we set the lattice space to be unity.

Let us discuss the order-disorder transition in $H>H_c$. Since a simple cubic lattice is considered, we can set up the "subchain" mean fields as $\boldsymbol{S}_{n,j}=\boldsymbol{M}_n+\delta\boldsymbol{S}_{n,j}$, where $\boldsymbol{M}_n$ is a classical vector field. We assume IC oscillation of the magnetization of the z component around the uniform(average) magnetization,

$$\boldsymbol{M}_n=[M_z\pm m_{ic}\cos(2k_Fn)]\boldsymbol{e}_z, \tag{4}$$

where m_{ic} is the amplitude of the IC fluctuation around the average magnetization M_z and the sign depends on the subchain. Also, for the transverse staggered fluctuation, we assume

$$\boldsymbol{M}_n=M_z\boldsymbol{e}_z\pm(-)^n m_s\boldsymbol{e}_x, \tag{5}$$

where m_s is the amplitude of the staggered magnetization in the transverse direction. Then a mean-field treatment of the interchain coupling yields the mean-field Hamiltonian per chain as

$$\mathcal{H}_{\mathrm{MF}}=\mathcal{H}_{1\mathrm{D}}+\mathcal{H}'_{ic/s} \tag{6}$$

where

$$\mathcal{H}_{1\mathrm{D}}\equiv\sum_n J(\boldsymbol{S}_n\cdot\boldsymbol{S}_{n+1})_\Delta-\bar{H}\sum_n S^z_n \tag{7}$$

is the 1D XXZ chain in an effective magnetic field $\bar{H}$ and $\mathcal{H}'_{ic/s}$ is the perturbation originating from the mean fields. For the IC order, we have $\bar{H}\equiv H-z\Delta J'M_z$ and

$$\mathcal{H}'_{ic}=-h_{ic}\sum_n\cos(2k_Fn)S^z_n+\mathrm{const}, \tag{8}$$

where $h_{ic}\equiv z\Delta J'm$. Note that the coordination number is $z=4$ for 3D. These effective fields should be determined self-consistently. Also, for the transverse staggered fluctuation, we have $\bar{H}\equiv H-z\Delta J'M_z$ and

$$\mathcal{H}_s=-h_s\sum_n(-)^nS^x_n+\mathrm{const} \tag{9}$$

with $h_s\equiv zJ'm_s$.

In order to treat the IC nature in the mean-field Hamiltonian, it is useful to employ an effective model in the continuum limit. This is achieved by the standard bosonization scheme.[12] Assuming $\bar{H}-H_c\gg h_{ic}$ or h_s, we can write the XXZ chain in the magnetic field as

$$\mathcal{H}_{1\mathrm{D}}\to\frac{v}{2}\int dx[(\partial_x\phi)^2+(\partial_x\theta)^2], \tag{10}$$

where v is the spin wave velocity and the compactification radius R is defined by the boundary condition $\phi(x+L)=\phi(x)+\pi RN$. The equal-time commutator of the bosonic fields is defined as $[\phi(x),\theta(y)]=i\Theta(x-y)$, where $\Theta(x-y)$ is the step function. For the XXZ model, the radius varies, $R=1/\sqrt{\pi}\to 1/\sqrt{4\pi}$, as the magnetic field increases from H_c to the saturation (free-fermion) limit. The TL exponent is given by $\eta=2\pi R^2$.

The boson representation of the spin operators is given by the formulas

$$S^z_n\simeq M_z+\frac{\partial_x\phi(n)}{2\pi R}+a\cos\left(\frac{\phi(n)}{R}-2k_Fn\right), \tag{11}$$

$$S^+_n\simeq(-)^nbe^{i2\pi R\theta(n)}, \tag{12}$$

where a and b are nonuniversal coefficients depending on Δ and H. Using (11) and (12), the amplitude of the equal-time correlation function is given by $A_1=a^2/2$, $B_0=b^2/2$ with the regularization

$$\int_0^\infty dk\frac{e^{-\alpha k}}{k}(1-\cos kx)=\ln x, \tag{13}$$

where α is a cutoff parameter. Although the analytical expressions for these coefficients in the magnetic field are still unknown, the numerical values are available in Ref. 9, they play a crucial role in semiquantitative evaluation of the transition temperature, as will be seen later. Substituting (11) and (12) into (8) and (9), we obtain the boson field representation of the perturbations,

$$\mathcal{H}'_{ic}\to-ah_{ic}\int dx\cos\left(\frac{\phi}{R}\right), \tag{14}$$

$$\mathcal{H}'_s\to-bh_s\int dx\cos(2\pi R\theta), \tag{15}$$

where we have omitted the $2k_F$ and $4k_F$ oscillating terms.

Let us consider the effects of $\mathcal{H}_{ic/s}$ on the Hamiltonian (10). The gap generated by the staggered field (15) was analyzed in Ref. 13 to be $\Delta E_s\sim h_s^{2/(4-\eta)}$. Also, for the operator of $\cos(\phi/R)$, a similar standard renormalization group argument leads to $\Delta E_{ic}\sim h_{ic}^{2/(4-1/\eta)}$. Both of the operators are always relevant between H_c and the saturation field. In the lower-field region, however, $\eta>1$ and thus $2/(4-1/\eta)<2/(4-\eta)$; The IC field is more relevant in the low-field region, while the transverse staggered field is more relevant in the high-field region. The border is just $\eta=1$, namely, an effective SU(2) point. For the case of $\Delta=2$, it corresponds to $H/J\simeq 1.5$ as in Fig. 1. This analysis of the gap is consistent with the naive expectation of the critical exponent η, which leads to IC order in the low-field region. For a quantitative analysis, however, the coefficients of the

gaps become important. It should also be noted that the assumption $\bar{H}-H_c \gg h_{ic}, h_s$ is not valid in the vicinity of the lower critical field.

Now we proceed to finite-temperature behaviors. In the framework of the mean-field theory, h_{ic} or h_s should be determined self-consistently. We write the IC magnetization of (6) at T, $\bar{H}$, and h_{ic} as $f_{ic}(T,\bar{H},h_s)$, and the staggered magnetization at T, $\bar{H}$, and h_s as $f_s(T,\bar{H},h_s)$. The self-consistent equations are written as $m_{ic}=f_{ic}(T,\bar{H},h_{ic})$ and $m_s=f_s(T,\bar{H},h_s)$, combined, respectively, with $h_{ic}=z\Delta J' m_{ic}$ and $h_s=zJ' m_s$. Taking the $h_{ic}, h_s \to 0$ limits, we can determine the transition temperatures

$$\frac{1}{zJ'\Delta} = \chi_{ic}, \quad \frac{1}{zJ'} = \chi_s, \tag{16}$$

where $\chi_{ic} \equiv \partial f_{ic}/\partial h_{ic}|_{h_{ic}=0}$ and $\chi_s \equiv \partial f_s/\partial h_s|_{h_s=0}$. According to the linear response theory, the dynamical susceptibility can be represented through the correlation function: $\chi_{\alpha\beta}(q,\omega;T)=-i\Sigma_n \int dt e^{i\omega t - iqn}\Theta(t)\langle[S^\alpha(n,t),S^\beta(0,0)]\rangle_T$, where $\langle\cdots\rangle_T$ denotes the average at a temperature T. For the TL Hamiltonian (10), this dynamical susceptibility was actually calculated in Refs. 12 and 14. For the estimation of the transition temperature, the susceptibility in the soft mode is essential: for the IC order, $\omega=0$ and $q=2k_F$, and for the staggered order, $\omega=0$ and $q=\pi$. Taking account of (13), the explicit form of the leading term becomes

$$\chi_{ic} = \chi_{zz}(2k_F,0;T) = \frac{A_1}{v}\sin\left(\frac{\pi}{2\eta}\right)\left(\frac{2\pi T}{v}\right)^{1/\eta-2} B\left(\frac{1}{4\eta},1-\frac{1}{2\eta}\right)^2, \tag{17}$$

$$\chi_s = \chi_{xx}(\pi,0;T) = \frac{B_0}{v}\sin\left(\frac{\pi\eta}{2}\right)\left(\frac{2\pi T}{v}\right)^{\eta-2} B\left(\frac{\eta}{4},1-\frac{\eta}{2}\right)^2, \tag{18}$$

where $B(x,y)$ is Euler's beta function. Note that the cutoff parameter in (17) and (18) formally corresponds to $\alpha=1$, due to the regularization (13). The magnetic-field dependence is implicitly included in v, η, A_1, and B_0. Substituting the above susceptibilities into (16), we obtain the final result for the transition temperatures:

$$T_c^{(ic)} = \frac{v}{2\pi}\left[z\Delta J' A_1 \frac{\sin(\pi/2\eta)}{v} B\left(\frac{1}{4\eta},1-\frac{1}{2\eta}\right)^2\right]^{\eta/(2\eta-1)}, \tag{19}$$

$$T_c^{(s)} = \frac{v}{2\pi}\left[zJ' B_0 \frac{\sin(\pi\eta/2)}{v} B\left(\frac{\eta}{4},1-\frac{\eta}{2}\right)^2\right]^{1/(2-\eta)}. \tag{20}$$

In the above expression, η and v can be exactly calculated by solving the Bethe ansatz integral equation as in Fig. 1. In addition, the nonuniversal amplitudes A_1 and B_0 can be obtained by using the density matrix renormalization group and the bosonization expression of the correlation function for the open boundary system.[9] We can thus calculate T_c quantitatively without any additional parameter. Here it should be noted that the previous estimation for $T_c^{(s)}$ was based on the correlation amplitude at zero magnetic field for $\Delta \leqslant 1$.[11]

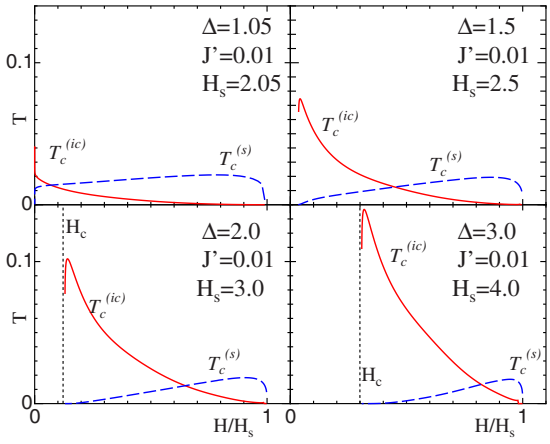

FIG. 2. (Color online) Transition temperatures for $\Delta=1.05$, 1.5, 2.0, and 3.0 with $J'=0.01$. The intrachain coupling J is set to unity. The solid and broken lines, respectively, represent $T_c^{(ic)}$ and $T_c^{(s)}$. The vertical dotted lines for $\Delta=2.0$ and 3.0 indicate the critical field H_c. H_c for $\Delta=1.05$ and 1.5 is not shown here, since it is located in vicinity of $H=0$. The horizontal axis is normalized by the saturation field H_s.

III. RESULTS

A. Phase diagram

On the basis of (19) and (20), we calculate the magnetic-field dependences of the transition temperatures of $J'=0.01$ for various Δ. The correlation amplitudes are extracted from the correlation functions obtained via the density matrix renormalization group, as mentioned in the previous section. In Fig. 2, we show the resulting phase diagrams in the T-H plane, where the solid and broken lines, respectively, indicate (19) and (20), and the magnetic field is normalized by the saturation field H_s. The curve corresponding to the higher T_c is realized as an actual order-disorder transition. In the following, we concentrate on the order-disorder transitions between the critical field H_c and the saturation field H_s. Thus the z Néel phase of $M=0$ below H_c is not shown here explicitly. In addition, note that H_c for $\Delta=1.05$ and 1.5 is in vicinity of $H=0$ in the scale of Fig. 2.

In Fig. 2, we can see that IC order certainly occurs above the critical field H_c. For $\Delta=1.05$, the IC order appears in the vicinity of $H=H_c \simeq 0$. As Δ increases, the transverse staggered order is suppressed, while the IC order develops rapidly and the corresponding range of H extends to the higher-field region. An important feature of the IC order is that the field dependence of $T_c^{(ic)}$ illustrates a characteristic curve; $T_c^{(ic)}$ has a maximum near H_c, and it decreases rapidly as H increases. This shape of the phase boundary should be contrasted with the semicirclelike boundary for the field-induced staggered order in the coupled Haldane system. On further increasing H, the curves for $T_c^{(ic)}$ and $T_c^{(s)}$ intersect at a certain magnetic field, which is denoted as H^{*c} henceforth, and trans-

verse staggered order appears for $H_s > H > H^*$. We can also see that, as Δ becomes large, H^* shifts to the higher-field side.

The behaviors above are basically consistent with the argument based on the TL exponents of the *XXZ* chain, since the region of $\eta > 1$ appears above the critical field H_c and it extends rapidly to the higher-field side, as Δ is increased. However, it should be noted that H^* does not coincide with the effective SU(2) point $\eta = 1$. This is because $\eta = 1$ is achieved at the effective field theory level and thus $A_1 \neq B_0$ is permitted even at $\eta = 1$, in contrast to the isotropic Heisenberg chain at zero field having SU(2) symmetry at the spin operator level. Since the correlation amplitude A_1 has a larger value than B_0 (e.g., see Fig. 2 in Ref. 9), $T_c^{(ic)}$ is more enhanced than $T_c^{(s)}$, implying that H^* slightly shifts to the higher-field side of the effective SU(2) point. In this sense, the precise amplitudes are essential in the interchain mean-field theory. In addition, we can see that Δ in (19) is also a source of such an enhancement of the IC order.

We next discuss the interchain-coupling dependence of transition temperatures. According to Eqs. (19) and (20), the precise J' dependences are given by $T_c^{(ic)} \propto J'^{\eta/(2\eta-1)}$ and $T_c^{(s)} \propto J'^{1/(2-\eta)}$, so that the scale of the transition temperature naturally becomes large, as J' is increased. In particular, we can see that $T_c^{(ic)}$ is more easily lifted toward the higher-field region where $\eta < 1$, since, as mentioned above, the IC order is basically enhanced by the correlation amplitude A_1 and the anisotropy Δ. However, we should remark that such enhancement of $T_c^{(ic)}$ in the interchain mean-field theory does not always lead to a clear observation of the IC order for a larger J'; we need to pay special attention to the stability of the IC order. Let us recall that the spin-flop transition occurs for the case of spatially isotropic exchange coupling ($J = J'$), where the magnetization directly jumps from the z Neel phase of $M = 0$ to the transverse staggered ordered state. This suggests that the IC order becomes thermodynamically unstable beyond a certain critical J',[15] so that it is embedded in the magnetization jump. Unfortunately, the critical J' cannot be determined within the framework of the mean-field theory for the interchain coupling, since analytical calculation of the free energy is still a difficult task. In the next section, nevertheless, we shall show that stable IC order actually occurs in the experimental situation of $BaCo_2V_2O_8$.

B. Comparison with experiment

Let us discuss the field dependence of the transition temperature of $BaCo_2V_2O_8$. The basic parameters were determined by magnetization and ESR measurements.[3] The exchange coupling in the chain direction is given by $J \simeq 65$ K and the precise anisotropy parameter is $\Delta \simeq 2.17$. The critical field is $H_c \simeq 3.9$ T and the saturation field is about 23 T with $g = 6.2$. In addition, we have actually calculated the correlation amplitudes for $\Delta = 2.17$. In Fig. 3, the field dependence of the transition temperature for $J' \simeq 0.09$ K ($J'/J = 0.001\,38$) is illustrated, together with the experimental data, where the solid and broken lines indicate (19) and (20), respectively.

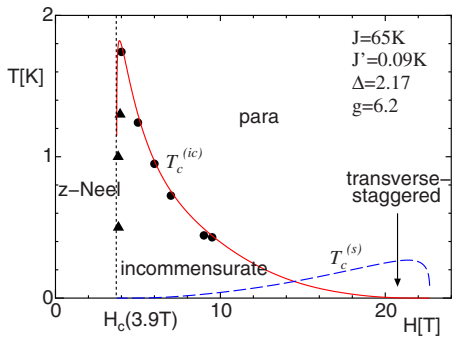

FIG. 3. (Color online) Transition temperatures for the IC and transverse staggered orders. The solid and the broken lines, respectively, represent $T_c^{(ic)}$ and $T_c^{(s)}$ for $\Delta = 2.17$ and $J'/J = 0.001\,38$. The vertical dotted line indicates $H_c = 3.9$ T. The solid circles indicate the experimentally observed transition temperature (Ref. 4) and the solid triangles mean the phase boundary between the z Néel order and the field-induced IC order.

In the left side, with H_c corresponding to the solid triangles, the z Néel order occurs at which the uniform magnetization is zero. Note that the transition temperature to the z Néel phase at $H = 0$ is about 5.4 K, which is much higher than $T_c^{(ic)}$. Above H_c, the z Néel order is destroyed by the magnetic field and then we come into the targeted region of the present theory. The solid circles indicate the experimental transition temperature up to 12 T. We can see that the theoretical curve (19) excellently reproduces the experimental results, implying the interchain mean-field theory is basically correct for 3D. A remarkable point is that the shape of the experimental phase boundary is consistent with the theoretical curve for IC order; as H increases above H_c, $T_c^{(ic)}$ decreases rapidly from $T \simeq 1.7$ down to 0.4 K. The above facts support the idea that the IC order driven by the one-dimensionality can be thermodynamically stabilized in the experimental situation. Another interesting point is that, on further increasing H, the theoretical curves for $T_c^{(ic)}$ and $T_c^{(s)}$ intersect at $H^* \simeq 15.1$ T, which predicts that transverse staggered order appears above $H \simeq 15.1$ T. In order to verify the theory, a specific heat measurement in a higher field is highly desirable. However, the value of $T_c^{(s)}$ is relatively low and thus the experimental observation in the competing region may be difficult.

IV. SUMMARY AND DISCUSSIONS

We have discussed field-induced IC order on the basis of bosonization combined with mean-field theory for the interchain interaction. In particular, the numerically exact correlation amplitudes play a crucial role in explaining the shape of the experimental phase boundary. In order to investigate the IC order beyond the mean-field level, we have also performed quantum Monte Carlo (QMC) simulations based on the directed loop algorithm. Then we confirmed that the IC order actually occurs for $J'/J = 0.1$.[16] We can therefore conclude that field-induced IC order is certainly realized in the actual system and the interchain mean-field treatment cap-

tures its essential nature. The interchain coupling of $BaCo_2V_2O_8$ estimated within the mean-field theory is $J' \simeq 0.09$ K.

From the theoretical point of view, the phase transition for the 3D classical spin model with easy-axis anisotropy was intensively studied in 1970s, in the context of the spin-flop transition.[17] The low-magnetization state is unstable in the 3D isotropic lattice system and the magnetization jumps directly from the z Néel to the spin-flopped state. The spin-flop transition also occurs for the 2D Ising-like XXZ model on the isotropic square lattice at zero temperature.[18] The present result implies that, as the 1D fluctuation is enhanced, the IC order—the spin version of the charge density wave (CDW)—emerges in the phase diagram. Of course, $BaCo_2V_2O_8$ is insulating, and thus the mechanism is attributed to the nesting of "spin" itself. In this sense, the present IC order is very similar to that in the spin-Peierls system.[19] However, the driving mechanism is the interchain spin-spin interaction itself rather than a spin-phonon coupling in the spin-Peierls case. Since the interchain interaction favors transverse staggered order as well, the spin-flop transition may be induced with a certain finite interchain coupling, implying that the thermodynamic stability of the IC order is a nontrivial question. The present result demonstrates that the IC order based on the 1D mechanism is certainly stabilized in the actual experimental situation. For the quasi-1D spin model, the Fermi wave number k_F can be easily controlled by the magnetic field, in contrast with the CDW in the metallic system. A further experimental study, particularly neutron scattering experiment in a magnetic field, would be highly interesting. In addition, the connection to the spin-flop transition in the high-field region is also a theoretically important problem, although the experiment for $BaCo_2V_2O_8$ suggests a weak first-order transition at H_c accompanying the spin-lattice coupling, which may cooperatively stabilize the incommensurate order.

Finally, we remark that our theory is valid not only for similar quasi-1D systems with easy-axis anisotropy, but also for a class of frustrated systems. In fact, frustrated systems are often mapped onto an effective XXZ model, for which IC order is actually known.[20,21] This enhancement of the IC fluctuation is also reported for an anisotropic $S=1$ chain.[22] We hope that the rich physics associated with spin anisotropy and quantum fluctuation can be developed by more theoretical and experimental research.

ACKNOWLEDGMENTS

We would like to thank S. Kimura, M. Sato, and N. Kawashima for valuable discussion. We are also grateful to T. Hikihara for providing the numerical data in Ref. 9. This work was partially supported by Grants in Aid for Science Research from MEXT, Japan. It was also supported by "High Field Spin Science in 100 T."

[1] T. Nikuni, M. Oshikawa, A. Oosawa, and H. Tanaka, Phys. Rev. Lett. **84**, 5868 (2000).
[2] Z. He, T. Taniyama, T. Kyomen, and M. Itoh, Phys. Rev. B **72**, 172403 (2005).
[3] S. Kimura, H. Yashiro, K. Okunishi, M. Hagiwara, Z. He, K. Kindo, T. Taniyama, and M. Itoh, Phys. Rev. Lett. **99**, 087602 (2007).
[4] S. Kimura, T. Takeuchi, K. Okunishi, M. Hagiwara, Z. He, K. Kindo, T. Taniyama, M. Itoh, arXiv:0707.3713 (unpublished).
[5] Z. Honda, H. Asakawa, and K. Katsumata, Phys. Rev. Lett. **81**, 2566 (1998).
[6] C. N. Yang and C. P. Yang, Phys. Rev. **150**, 321 (1966).
[7] F. D. M. Haldane, Phys. Rev. Lett. **45**, 1358 (1980).
[8] N. M. Bogoliubov, A. G. Izergin and V. E. Korepin, Nucl. Phys. B **275**, 687 (1986).
[9] T. Hikihara and A. Furusaki, Phys. Rev. B **69**, 064427 (2004).
[10] H. J. Schulz and C. Bourbonnais, Phys. Rev. B **27**, 5856 (1983); H. J. Schulz, Phys. Rev. Lett. **77**, 2790 (1996).
[11] S. Wessel and S. Haas, Phys. Rev. B **62**, 316 (2000).
[12] T. Giamarchi *Quantum Physics in One Dimension* (Oxford University Press, Oxford, 2004).
[13] M. Oshikawa and I. Affleck, Phys. Rev. Lett. **79**, 2883 (1997).
[14] H. J. Schulz, Phys. Rev. B **34**, 6372 (1986).
[15] This critical J' may depend on the magnetic field H.
[16] T. Suzuki, N. Kawashima, and K. Okunishi, J. Phys. Soc. Jpn. **76**, 123707 (2007).
[17] M. E. Fisher and D. R. Nelson, Phys. Rev. Lett. **32**, 1350 (1974); M. E. Fisher, *ibid.* **34**, 1634 (1975).
[18] M. Kohno and M. Takahashi, Phys. Rev. B **56**, 3212 (1997).
[19] M. C. Cross, Phys. Rev. B **20**, 4606 (1979).
[20] N. Maeshima, K. Okunishi, K. Okamoto and T. Sakai, Phys. Rev. Lett. **93**, 127203 (2004).
[21] T. Suzuki and S. I. Suga, Phys. Rev. B **70**, 054419 (2004).
[22] T. Sakai, Phys. Rev. B **58**, 6268 (1998).